

**THIS IS THE PEER REVIEWED VERSION OF
THE FOLLOWING ARTICLE:**

Volpe, V., D'Auria, M., Sorrentino, L., Davino, D., Pantani, R.
“INJECTION MOLDING OF MAGNETO-SENSITIVE POLYMER COMPOSITES”
Materials Today Communications
Volume 15, June 2018, Pages 280-287
DOI: 10.1016/j.mtcomm.2018.03.016

WHICH HAS BEEN PUBLISHED IN FINAL FORM AT
<https://www.sciencedirect.com/science/article/pii/S235249281830103X>

THIS ARTICLE MAY BE USED ONLY FOR NON-COMMERCIAL PURPOSES

Injection molding of magneto-sensitive polymer composites

Valentina Volpe^a, Marco D'Auria^{b,c}, Luigi Sorrentino^b, Daniele Davino^c, Roberto Pantani^a

^aDepartment of Industrial Engineering. University of Salerno

^bInstitute of Polymers, Composites and Biomaterials (IPCB - CNR), Portici (Na)

^cDepartment of Engineering. University of Sannio

* Corresponding author. Department of Industrial Engineering, University of Salerno, via Giovanni paolo

II 132, Fisciano, Salerno, Italy.

E-mail address: rpantani@unisa.it (R. Pantani).

ABSTRACT

Magneto sensitive parts made of a thermoplastic elastomer reinforced with iron microparticles were prepared by imposing a magnetic field during injection molding. In particular, an aluminum mold was designed to host an electro-magnet able to apply a magnetic field during the injection of the material into the mold and its subsequent solidification. Samples obtained in the presence of magnetic field were characterized by a peculiar, aligned distribution of iron particles along the magnetic field lines, and columnar structures of variable length were obtained. The mechanical characterization showed that the samples in which the iron particles were aligned had higher modulus compared to samples in which the particles were randomly dispersed. The magnetic field induced an anisotropic structural reinforcement that imparted to composite samples a magnetostrictive feature, namely the capability to sense the magnetic field and to react with a shape change under the application of the magnetic field.

Keywords

Injection molding, magnetic field, composites, mechanical characterization, magnetostriction

28 **1. Introduction**

29 Magneto-sensitive polymer composites are smart materials made by embedding magnetic
30 particles, micrometric or nanometric in size, into a polymeric matrix. In presence of a suitable
31 magnetic field, particles align themselves along magnetic field lines leading to an anisotropic
32 structural reinforcement. This alignment confers to the material the characteristic of being
33 “smart” in the sense it can react to an external stimulus by changing its properties in the desired
34 way.

35 In the scientific literature, several magnetorheological (MR) composites based on polymers and
36 aligned magnetic particles (MP) have been proposed [1]. Magnetorheological composites are
37 smart materials able to quickly, continuously and reversibly respond to the application of a
38 magnetic field external stimulus with a change in their properties [2-7]. These smart materials
39 can be fluid or solid [8-10]. MR fluids exhibit a field-dependent yield stress and are
40 conventionally used for vibration control and suspensions in the automotive field. Bastola et al.
41 in 2017 [11] developed a new type of hybrid magnetorheological elastomers (H-MREs) as a
42 combination of an MR fluid and an elastomer matrix by means of a 3D printing technology.
43 MR solids are usually prepared by mixing magnetic particles in viscous precursors of the solid
44 and, unlike the fluids, retain their shape after the molding process. They have field-dependent
45 stiffness and can be used in adaptive tuned variable-stiffness devices, soft actuators and artificial
46 muscles [12, 13]. They include magnetorheological gels [14-16], foams [17-20] and elastomers.
47 In the last decades several authors focused their attention on magnetorheological elastomers
48 (MREs), materials obtained by embedding micro-sized magnetizable particles in an elastomeric
49 matrix during the crosslinking process [21, 22]. The presence of a magnetic field during the
50 production of the elastomer object induces interactions between particles that promote an
51 anisotropic ordered configuration formed by particle chains aligned along the field direction.
52 Anisotropic MR elastomers with special chain structure of magnetic particles have attracted the
53 interest of the researchers and materials have been fabricated based on different matrices, i.e.
54 silicone elastomers, hard natural or synthetic rubber and polyurethane [23-27].

55 In 2003 Farade and Benine analyzed mechanical and magnetic properties of particle-filled
56 silicon rubber produced by aligning the embedded particles in the elastomer by the application
57 of a magnetic field when the cross-linking of the resin took place [22].

58 Guan et al. in 2008 [28] prepared and analyzed MRE consisting of carbonyl iron particles
59 displaced in a silicon rubber matrix. They proved that magnetostrictive effect (shape variation of
60 such materials during the application of a magnetic field) increases on increasing the volume
61 fraction of particles. Magnetostriction generally increases with increasing magnetic field and
62 orientation of particles influences the magnetostrictive performance significantly. In 2010 Wu et
63 al. [29] investigated the influences of carbonyl iron particle content on the microstructure,
64 thermal, mechanical and MR properties of PU MREs. They found that the chain-like structures,
65 obtained by alignment of the particles according to the magnetic field lines, becomes denser as
66 the iron content increases. Furthermore, they demonstrated that the orientation of carbonyl iron
67 particles can greatly enhance the compressive strength of the composite, but the tensile
68 properties of PU MREs decrease. In 2017 Perales-Martínez et al. [30] studied the rheological
69 and mechanical properties of magnetorheological elastomer based on silicone rubber with
70 different contents of carbonyl iron micro-particles. They found that the enhancement of the
71 mechanical properties was achieved with the adding of 20% of carbonyl iron particles to the
72 silicon rubber matrix, obtaining up to 111% of additional stretch and 95% of increment in
73 tensile strength compared to that of the bare material.

74 Until now, to these authors' knowledge, only magneto-sensitive elastomers produced by curing
75 the magnetizable particles/elastomeric matrix mixtures in presence of a magnetic field have
76 been proposed [31]. In this work, the combination of magneto-sensitive elastomers concept to
77 the injection molding process is proposed. In fact, among polymer processing technologies,
78 injection molding allows large scale productions of 3D articles. The idea behind this work
79 involves the use of injection molding technology in order to make profit of its main advantage:
80 the ability to give arbitrary and complex shapes to the artifacts. In this way, if the polymer
81 viscosity is low enough, magnetic particles can be aligned by the application of an external

82 magnetic field. Gradients of mechanical properties inside the injection molded parts can be
83 obtained depending on the intensity and the magnetic field direction. To this aim, a special mold
84 has been designed and a preliminary rheological study has been made in order to choose the
85 elastomer suitable for the purpose.

86

87 **2. Materials and methods**

88 A polyolefin elastomer, Engage 8402 supplied by DuPont Dow Elastomers (Midland, Michigan,
89 USA) was adopted in this work. Engage is an ethylene-octene copolymer that performs well in a
90 wide range of thermoplastic elastomer applications. The properties of the adopted polymer are
91 reported in Table 1.

92

93 **Table 1**

94 Properties of Engage 8402 as provided by the supplier.

| Property | Method | Unit | Typical value |
|---------------------------------|-------------------------------------|-------------------|---------------|
| Melt Flow Index (190°C/2.16 kg) | ASTM D-1236 | dg/min | 30 |
| Total Crystallinity | - | % | 34 |
| Melt Temperature | DSC Melting Peak (Rate 10°C/min) | °C | 96 |
| Glass Transition Temperature | DSC Inflection Point | °C | -44 |
| Flexural Modulus (2% Secant) | ASTM D-790 | MPa | 69.9 |
| Density | ASTM D-792 | g/cm ³ | 0.902 |

95

96 Carbonyl Iron Powder CIP SQ supplied by Basf (Ludwingshafen, Germany) was adopted as
97 filler in this work. These particles have performed well for magneto-sensitive polyurethane
98 foams [31]. The main properties of the adopted Carbonyl Iron Powder are: minimum Fe content

99 99.5 %, maximum C content 0.05 %, maximum C content 0.22 %, mean particle size lower than
100 10 microns.

101

102 *2.1 Masterbatch preparation and Rheological measurements*

103

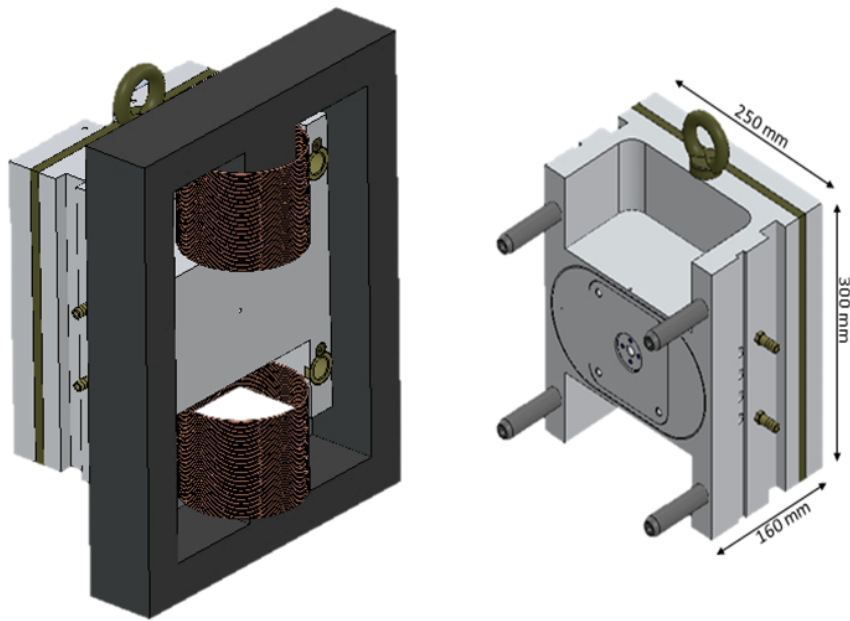
104 A masterbatch with 50 % by weight of iron microparticles (particle size -325 meshes, assay
105 97%), supplied by Sigma Aldrich (Saint Louis, Missouri, USA) was produced with Engage
106 8402 by means of a twin screw extruder (type PTW100 from Haake Thermo GmbH, Germany).
107 Subsequently, in order to obtain a compound with 20 % by weight of iron particles, the
108 masterbatch was diluted with neat polymer directly in the injection molding machine. The
109 extrusions were conducted at 160°C, while the die temperature was set at 130°C.

110 Rheological properties were studied by means of a Haake Mars rotational rheometer (Thermo
111 Haake GmbH, Germany), rheological tests were performed on the neat Engage 8402 and
112 Engage 8402+50% Fe by weight (10% by volume) to select the best processing conditions.
113 These tests were carried out at different temperatures (160 °C, 180 °C and 200 °C) thus
114 obtaining the dependence of the complex viscosity, G' and G'' on the oscillation frequency.

115

116 *2.2 Injection molding*

117 A 70-ton Negri-Bossi injection molding machine (CANBIMAT 65/185, from Negri-Bossi SpA,
118 Italy) with a screw diameter of 25 mm and L/D=22 was used in this work. Clamping unit of the
119 injection molding machine consists of an aluminum mold expressly designed to host an
120 electromagnet which generates a magnetic field in the cavity (Figure 1).



121

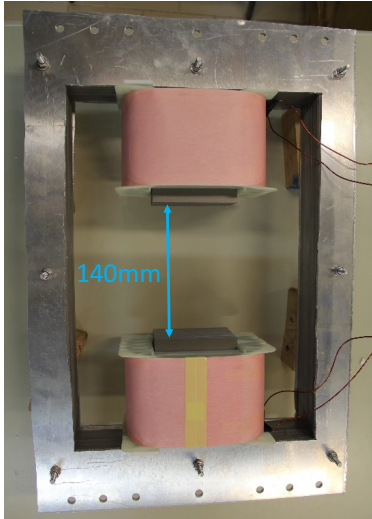
122 **Fig. 1.** Sketch of the Aluminum mold with the custom electromagnet.

123

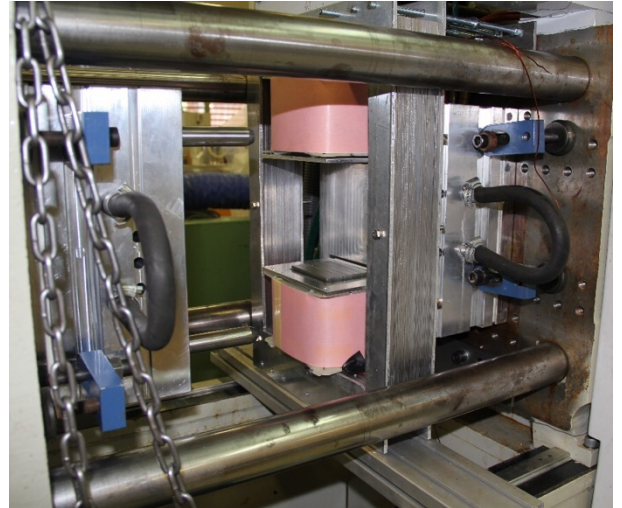
124 Aluminum is chosen because it does not interfere with the magnetic field and allows to preserve
125 the spatial distribution of the magnetic field lines, in order to exploit them to properly align the
126 reinforcing particles. The magnetic field time profile was optimized to properly move the iron
127 particles in linear aggregates just before the polymer consolidation during cooling in the mold.

128 The electromagnet (Figure 2), fixed to the stationary platen of the injection molding machine,
129 consists of two coils of copper wires windings (copper wire diameter 1.4 mm, tolerance 2 mm,
130 winding resistance is 6.7 Ohm) connected to a power supply (EA-PSI 8360-10 T) and a
131 laminated magnetic core to form an “iron circuit” for the magnetic field lines. The dimensions
132 of the electromagnet are a trade-off among magnetic performance, maneuverability and safe
133 operations of the injection molding machine, as shown in Fig. 2b.

134



a



b

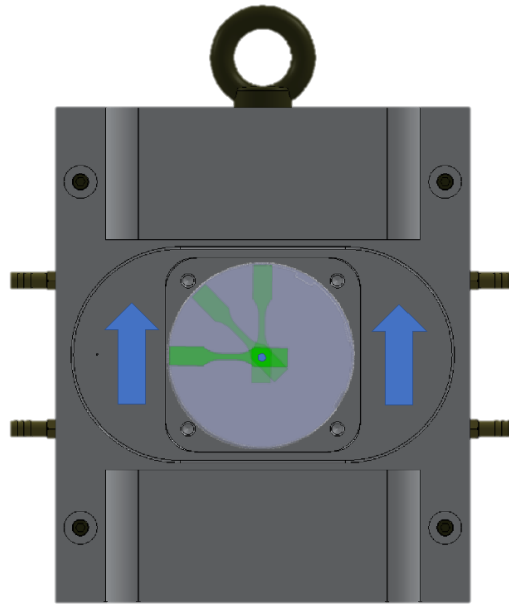
135 **Fig. 2.** a) Custom Electromagnet with a 140 mm airgap; b) aluminum mold hosting the
136 electromagnet

137

138 The magnetic core is laminated in order to avoid eddy currents effects. The iron sheets are
139 standard M300-35A ISO. Number of spires and geometry of the magnetic core allow to obtain a
140 magnetic flux of 1.3 mWb.

141 The cavity with dumbbell geometry is obtained on a circular insert mounted on the moving
142 mold. The dumbbell cavity, 3 mm thick, was dimensioned according to the Type V of ASTM D
143 638-03. The rotation of the circular insert allows to orient the dumbbell sample at different
144 angles with respect to the magnetic field lines (Figure 3).

145



146

147 **Fig. 3.** Moving mold with dumbbell geometry obtained on a circular insert. The blue arrows
148 refer to the direction of the MF given by the custom electromagnet.

149

150 This would lead to iron particles aligned with different angles with respect to the dumbbell main
151 axis (which coincides with the flow direction during molding), thus inducing different
152 mechanical and magneto-mechanical properties. In this work, the dumbbell samples were
153 molded with the main axis of the sample oriented at 0 degree, 45 degree and 90 degree with
154 respect to the magnetic field orientation (Figure 3). The samples will be coded according to this
155 feature so that “NoMF” will refer to a sample molded without magnetic field and “MF X°” will
156 refer to a sample molded with the main axis of the dumbbell oriented at X° degrees with respect
157 to the Magnetic Field direction. The experimental conditions adopted during the injection
158 molding process are reported in Table 2.

159

160 **Table 2**

161 Processing condition for injection molding.

| | |
|---|-----------------------|
| Temperature profile [°C] (increasing distance from the hopper to the nozzle) | 200 - 210 - 220 - 220 |
| Nozzle temperature [°C] | 220 |
| Mold temperature [°C] | 45 |
| Filling pressure (hydraulic system) [bar] | 70 |
| Screw rotation speed [rpm] | 100 |
| Back pressure (hydraulic system) [bar] | 2 |
| Injection speed [%] | 30 |
| Shot size [cm³] | 2.3 |
| Cooling time [s] | 60 |
| Iron content [% by weight] | 20 - 50 |
| Working current [A] | 8 - 9 |
| Working voltage [V] | 115 - 120 |
| Magnetic field “ON” time [s] | 10 |

162

163 During the injection molding process, at the beginning of the injection phase, the power supply
164 is switched on so that the desired magnetic field is generated. The magnetic field is kept active
165 for 10 seconds, in order to allow the orientation of the iron particles within the molten polymer.

166

167 *2.3 Scanning electron microscopy*

168 After production, the samples were sectioned and analyzed by a LEO-EVO 50 Scanning
169 electron microscope (Zeiss, Germany) in order to observe the spatial distribution of iron
170 particles in the polymeric matrix. The section observed by scanning electron microscopy is the
171 central part of the narrow section.

172

173 2.4 Mechanical properties

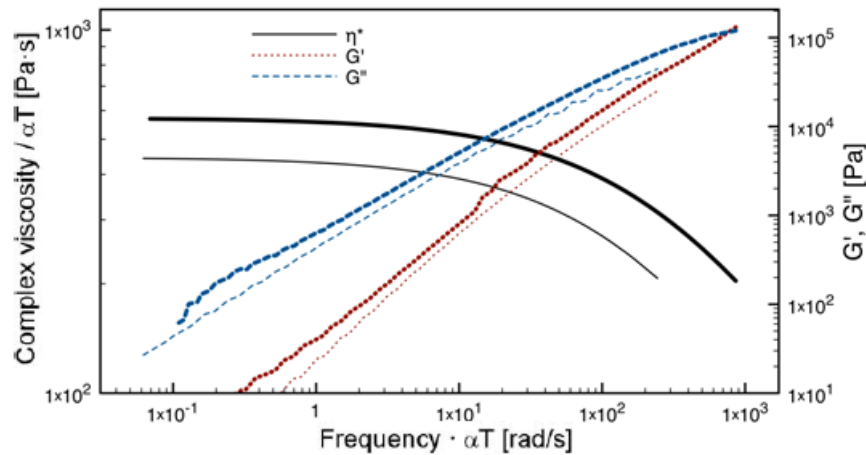
174 Mechanical properties of the samples have been tested by a 5kN universal testing machine
175 (LRXplus, Lloyd, United Kingdom). Self-tightening grips (model TH243-20 from DGTS, Italy)
176 have been used for tensile tests with a column speed of 10mm/min. The internal load cells and
177 extensimeter have been used to measure forces and deformations.

178

179 3. Results

180 The rheological properties of neat Engage and Engage 8402+50% Fe by weight are shown in
181 Fig. 4, in which it is possible to note that 50% by weight of iron powder results in increased
182 viscosity of the material. The rheological results obtained at three temperatures (160°C, 180°C,
183 200°C) have been superposed, using an appropriate shift factor for each temperature, to obtain a
184 master curve. The shift factors (αT) used to make the master curves of pure Engage and
185 Engage+50%_w Fe are reported in Table 3.

186



187

188 **Fig. 4.** Rheological properties of neat Engage (thin lines) and Engage 8402+50% Fe by weight
189 (thick lines). Mastercurves at 180°C

190

191 **Table 3**

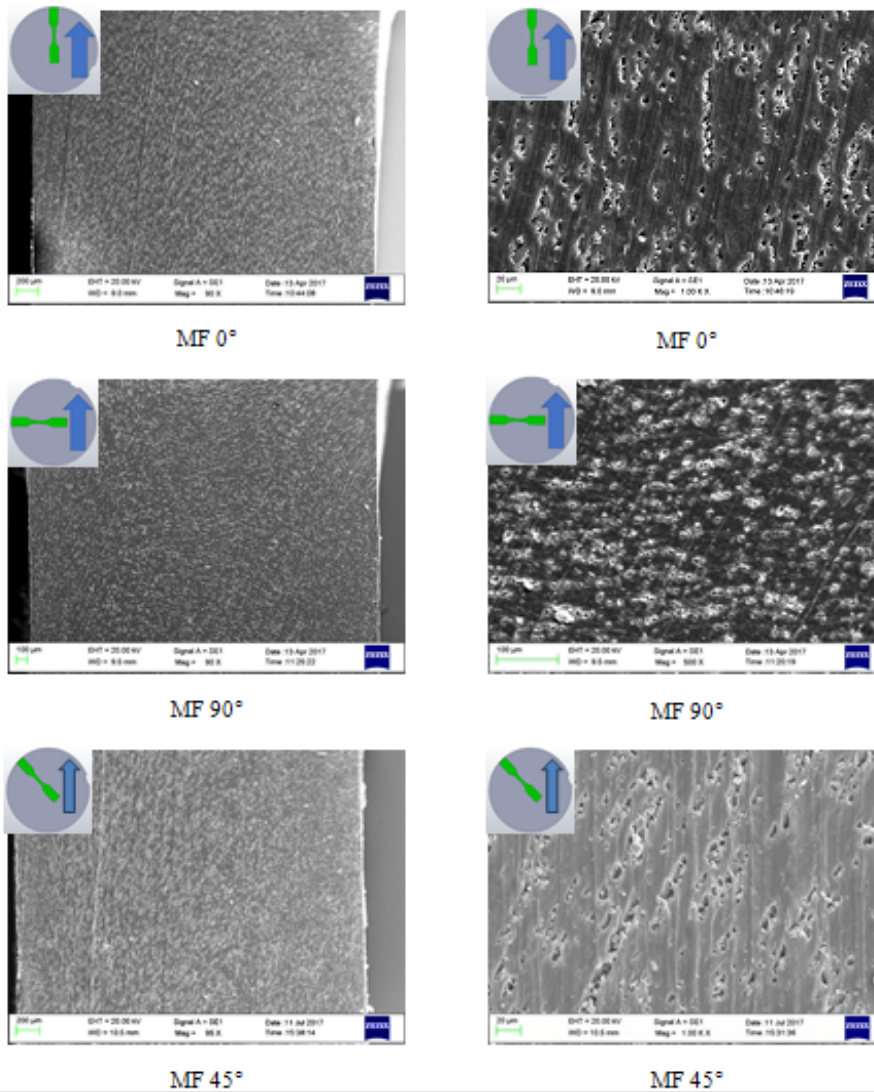
192 Shift factors of the mastercurves of pure Engage and Engage+50%_w Fe.

| Temperature [°C] | Shift factor Pure Engage | Shift factor Engage+50%_w Fe |
|-------------------------|---------------------------------|---|
| 160 | 1.66 | 1.85 |
| 180 | 1 | 1 |
| 200 | 0.62 | 0.69 |

193

194 Samples obtained by injection molding with the application of a magnetic field were observed
195 by SEM in order to verify the degree of orientation of the particles. Figure 5 shows the
196 micrographs of the Engage 8402+Fe 50% by weight obtained by orienting the dumbbell at 0°,
197 45° and 90° with respect to the direction of the magnetic field. The micrographs on the left
198 show the entire section of the sample, while those on the right side show a magnification of the
199 very central part of the corresponding image on the left.

200



201

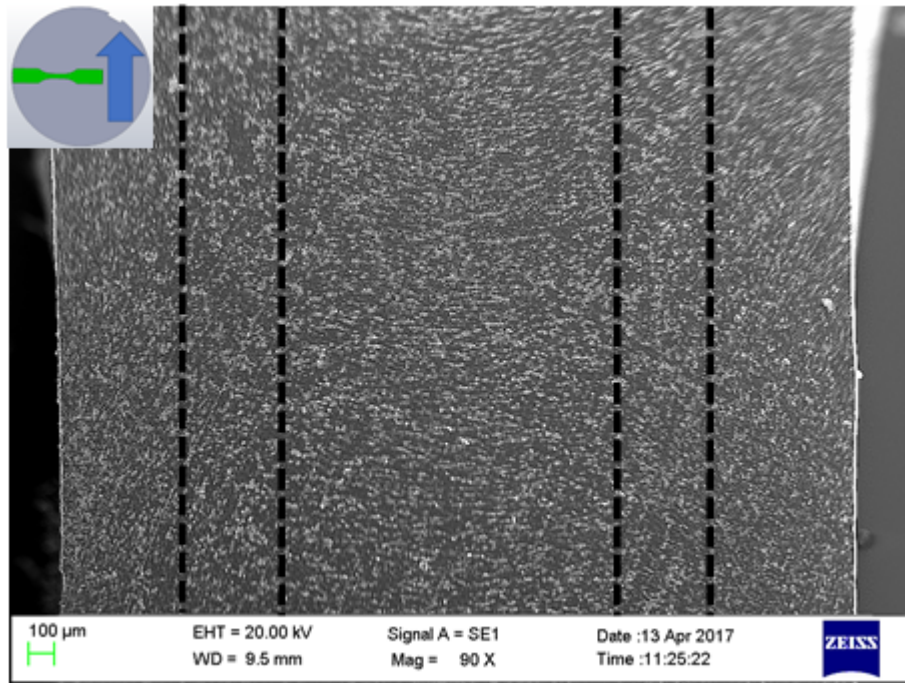
202 **Fig. 5.** SEM micrographs of Engage 8402+Fe 50% by weight obtained by orienting the
 203 dumbbell at 0°, 45° and 90° with respect to the direction of the magnetic field.

204

205 The images confirm that the iron particles are indeed oriented along the magnetic field
 206 direction, developing chain-like structures. The spatial arrangement of particles in the three
 207 different cases is also clearly visible: the chains are directed along a direction that exactly
 208 corresponds to the direction of the magnetic field during molding. Furthermore, the observation
 209 of the entire section of the sample allows the identification of distinct zones (Fig. 6): a central
 210 zone oriented in the direction of the magnetic field, an outer area that exhibits a random
 211 distribution of the particles, a partially oriented intermediate zone. This result may show that, in

212 perspective, it is possible to obtain different orientation of particles and morphology within the
213 same molded part.

214



216 **Fig. 6.** Engage 8402+Fe 50% by weight, MF 90°: subdivision of the section into an oriented
217 central zone, an outer area with random distribution of the particles, a partially oriented
218 intermediate zone.

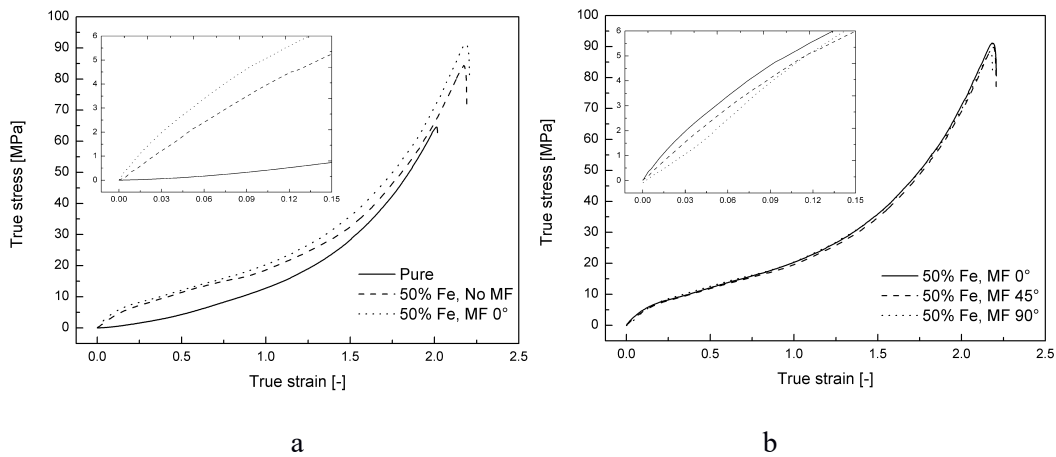
219

220 This spatial arrangement of particles is closely related to the temperature profile of the polymer
221 melt inside the cavity. In particular, since the solidification proceeds from the sample surface
222 toward the core, the internal layers remain at high temperatures for a longer time. The low
223 temperature of the polymer melt in the outer area implies high viscosity, and thus the action of
224 the magnetic field is not sufficient to allow an orientation and the particles are distributed
225 without a particular order within the polymer.

226 The presence of aligned particles in chain form can also be detected by placing the molded
227 sample, free to move, under a magnetic field. In fact, when the magnetic field is activated, the
228 sample instantly respond by moving and stopping in a position where the particle chains inside

229 are perfectly aligned with the applied magnetic field lines, similarly to a compass needle. The
 230 position that the samples take under a magnetic field indirectly confirms the effective alignment
 231 of the iron particles along the designed angle. Also NoMF samples instantly respond to the
 232 application of a magnetic field, but the direction is always that of the main flow during molding
 233 (namely MF 0°). This phenomenon is probably due to the fact that, even in absence of magnetic
 234 field during the foam injection, the iron particles can assume a certain anisotropic distribution,
 235 hence some degree of orientation, due to the flow.

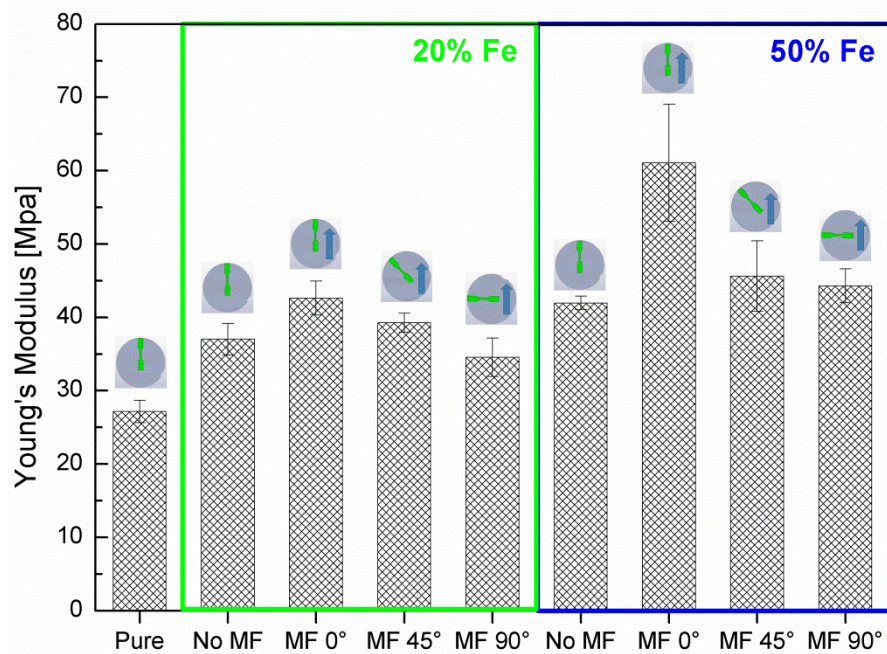
236 The mechanical properties of samples were characterized in tension mode, in order to evaluate
 237 the stiffness and the strength as function of the reinforcement spatial distribution. Figure 7
 238 shows the stress-strain curves obtained by tensile test on pure Engage, Engage with 50% Fe by
 239 weight without magnetic field (50% Fe, No MF) and Engage with 50% Fe oriented at 0°. Since
 240 the values of strain are considerable, the curves are expressed in terms of “true stress” and
 241 “true strain”. In particular, if L is the current length of the gage, L₀ is its initial value, P is the
 242 load and A₀ is the initial cross-sectional area, the “true strain” was calculated as $\epsilon = \ln(L/L_0)$ and
 243 the “true stress” as $\sigma = P/A_0 L/L_0$.



246 **Fig. 7.** Stress-strain curves of pure Engage, Engage with 50% Fe by weight without magnetic
 247 field (50% Fe, No MF) and Engage with 50% Fe oriented at 0° (50%Fe, MF 0°) (a); stress-
 248 strain curves of Engage with 50% Fe oriented at 0°, 45° and 90° (b).

249

250 The slope of the initial linear portion of the stress-strain curves represents the Young's modulus
251 of the tested material. Figure 8 shows the Young's modulus of pure Engage, Engage with 20%
252 and with 50% Fe by weight.



253

254 **Fig. 8.** Young's modulus of pure Engage and Engage with 20% and 50% by weight of iron
255 particles oriented at 0°. 45° and 90° with respect to the magnetic field direction.

256

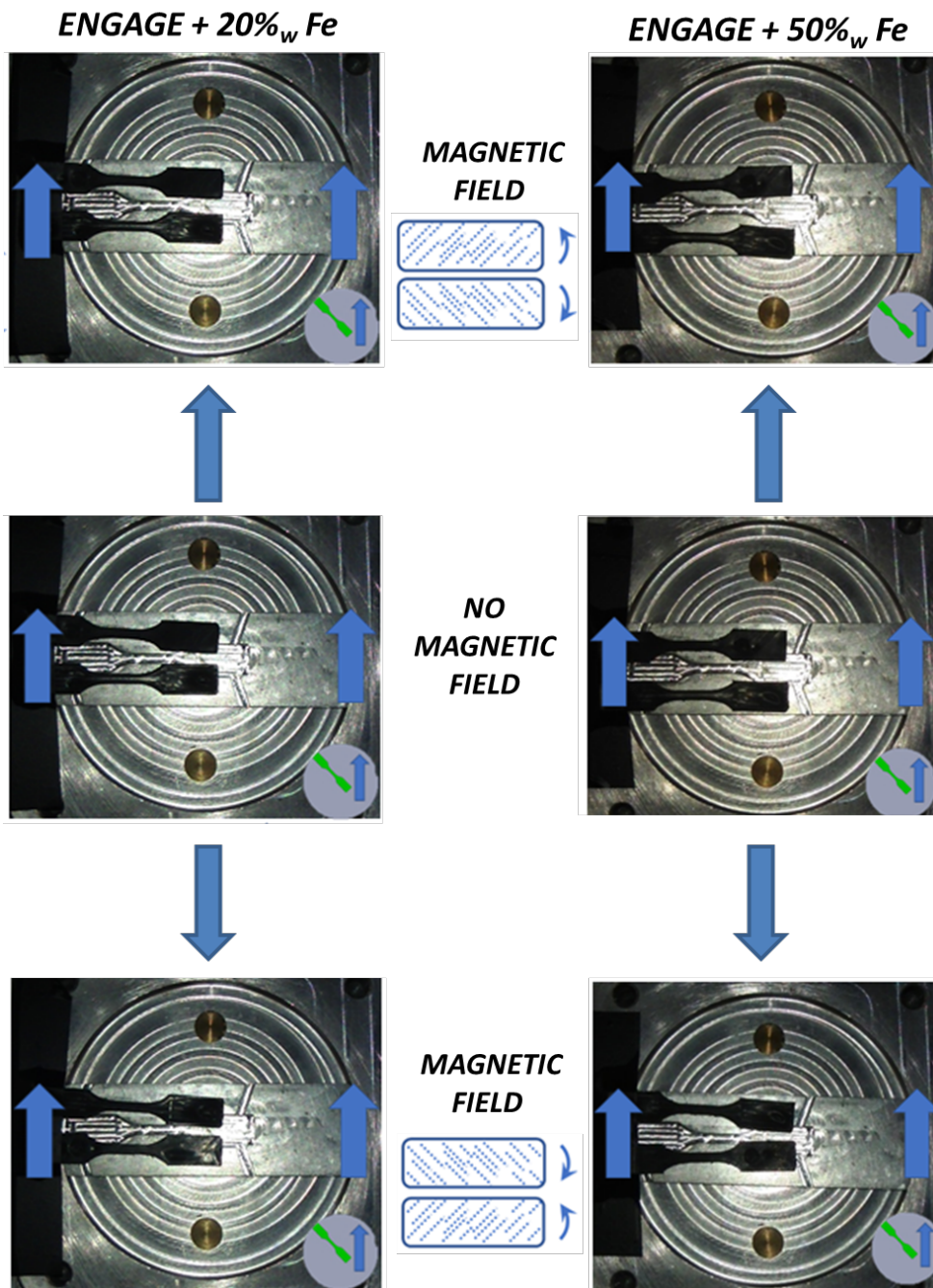
257 Results without the application of any magnetic field and with magnetic field at 0°, 45° and 90°
258 with respect to the flow direction are reported. It is possible to observe that the addition of iron
259 particles increases the Young's modulus, and that it is higher in case of magnetic field at 0° with
260 respect to the flow direction. In particular, the Young's modulus of Engage with 50 wt% and MF
261 at 0° is 33% higher than that measured on NoMF sample with the same iron content.

262

263 *Magnetostrictive behaviour*

264 Samples injection molded at 45° with respect to the magnetic field direction were subjected to
265 further tests, in order to evaluate their smart “active” behavior. In particular, the custom
266 electromagnet was used and two MF 45° samples were positioned in the center of the magnetic
267 field and blocked on one side. When the magnetic field is activated, the two samples tend to

268 deform by aligning the chain-like structures along the direction of the magnetic field, thus
269 inducing a shape change. Samples are deformed upwards or downwards depending on the actual
270 direction of the particles inside them (see the scheme reported in Fig. 9, which shows the
271 response of samples with 20 wt% and 50 wt% of Fe under a MF set at 45°). It is possible to
272 observe that the samples with 20 wt % of Fe undergo an almost imperceptible deformation (Fig.
273 9, left), so the particle orientation is not enough to induce visible deformation. Vice versa, the
274 samples with 50 wt% of Fe (Fig. 9, right) undergo a visible deformation due to the tendency of
275 the chain-like structures to align with the magnetic field lines. In particular, they tend to bend to
276 move apart in one case (top pictures in Fig. 9) or to get closer in the other case (bottom pictures
277 in Fig. 9). This proved that the presence of chain-like structures induces a magnetostrictive-like
278 behavior in the injection molded samples, phenomenon applicable in valves or pumps design.
279



280

281 **Fig. 9.** Magneto-sensitivity tests on samples of Engage+20% Fe by weight (left) and
 282 Engage+50% Fe by weight (right) with MF 45°. The schemes indicate the direction of the
 283 particles inside the samples.

284

285

286 **5. Conclusions**

287 In this work, composite lightweight materials based on a polymeric matrix with embedded
288 magnetic micro-particles have been developed by using a thermoplastic elastomer mixed with
289 iron microparticles.

290 A new aluminum mold was designed and built in such a way to host an electromagnet, able to
291 impose a magnetic field during the injection of the material into the cavity and its subsequent
292 solidification.

293 The application of the magnetic field during the injection molding process allowed the
294 formation of columnar aggregates oriented along the magnetic field lines, which were clearly
295 visible by SEM.

296 These oriented structures make the samples able to orient, if placed in a magnetic field, in the
297 same direction of the magnetic field imposed during injection molding, like the needle of a
298 compass. It was also noticed that the system obtained without the application of a magnetic field
299 also responded to the application of a magnetic field due to some flow-induced orientation in
300 the direction of flow. This phenomenon was interpreted by considering that the iron particles
301 can assume a certain anisotropic distribution, hence some degree of orientation, due to the flow
302 of the polymer after entering the mold. It was observed that the addition of iron particles
303 increases the Young's modulus, which is even higher in case of magnetic field at 0° with respect
304 to the flow direction.

305 It was verified that the peculiar particle distribution imparted to the samples a magnetostrictive
306 behavior, namely the ability to change shape in presence of an external magnetic field. This
307 property may be exploited in several ways, such for instance in the production of valves or
308 pumps activated in a contactless way by means of a magnetic fields.

309

310 **Acknowledgements**

311 These research activities were supported by the Italian Ministry of Education and Research
312 (MIUR) within the PRIN project developing polymeric smart foams with behavior controlled by

313 the magnetic field – E.PO.CA.M. (grant number PRIN 2012JWPMN9). The authors gratefully
314 acknowledge Antonio Vecchione and Rosalba Fittipaldi from CNR-SPIN and Dept. of Physics
315 “E. R. Caianiello”, University of Salerno, for their technical support in scanning electron
316 microscopy analysis.

317

318 The raw/processed data required to reproduce these findings cannot be shared at this time as the data also
319 forms part of an ongoing study.

320

321 **References**

322

323

- 324 [1] E. Galipeau, P.P. Castaneda, The effect of particle shape and distribution on the macroscopic behavior
325 of magnetoelastic composites, *Int J Solids Struct*, 49 (2012) 1-17.
- 326 [2] S. Bednarek, The giant linear magnetostriction in elastic ferromagnetic composites within a porous
327 matrix, *J Magn Magn Mater*, 301 (2006) 200-207.
- 328 [3] P. Blom, L. Kari, Amplitude and frequency dependence of magneto-sensitive rubber in a wide
329 frequency range, *Polym Test*, 24 (2005) 656-662.
- 330 [4] G. Diguët, E. Beaugnon, J.Y. Cavaille, From dipolar interactions of a random distribution of
331 ferromagnetic particles to magnetostriction, *J Magn Magn Mater*, 321 (2009) 396-401.
- 332 [5] L. Lanotte, G. Ausanio, V. Iannotti, G. Pepe, G. Carotenuto, P. Netti, L. Nicolais, Magnetic and
333 magnetoelastic effects in a composite material of Ni microparticles in a silicone matrix, *Phys Rev B*, 63
334 (2001).
- 335 [6] Y.L. Wang, Y.A. Hu, L. Chen, X.L. Gong, W.Q. Jiang, P.Q. Zhang, Z.Y. Chen, Effects of
336 rubber/magnetic particle interactions on the performance of magnetorheological elastomers, *Polym Test*,
337 25 (2006) 262-267.
- 338 [7] G.Y. Zhou, Z.Y. Jiang, Deformation in magnetorheological elastomer and elastomer-ferromagnet
339 composite driven by a magnetic field, *Smart Mater Struct*, 13 (2004) 309-316.
- 340 [8] S. Abramchuk, E. Kramarenko, D. Grishin, G. Stepanov, L.V. Nikitin, G. Filipcsei, A.R. Khokhlov, M.
341 Zrinyi, Novel highly elastic magnetic materials for dampers and seals: part II. Material behavior in a
342 magnetic field, *Polym Advan Technol*, 18 (2007) 513-518.
- 343 [9] X.L. Gong, C.Y. Guo, S.H. Xuan, T.X. Liu, L.H. Zong, C. Peng, Oscillatory normal forces of
344 magnetorheological fluids, *Soft Matter*, 8 (2012) 5256-5261.
- 345 [10] T. Mitsumata, S. Ohori, Magnetic polyurethane elastomers with wide range modulation of elasticity,
346 *Polym Chem-Uk*, 2 (2011) 1063-1067.
- 347 [11] A.K. Bastola, V.T. Hoang, L. Li, A novel hybrid magnetorheological elastomer developed by 3D
348 printing, *Mater Design*, 114 (2017) 391-397.
- 349 [12] H.X. Deng, X.L. Gong, L.H. Wang, Development of an adaptive tuned vibration absorber with
350 magnetorheological elastomer, *Smart Mater Struct*, 15 (2006) N111-N116.
- 351 [13] J.K. Wu, X.L. Gong, Y.C. Fan, H.S. Xia, Physically crosslinked poly(vinyl alcohol) hydrogels with
352 magnetic field controlled modulus, *Soft Matter*, 7 (2011) 6205-6212.
- 353 [14] G. Filipcsei, I. Csetneki, A. Szilagyí, M. Zrinyi, Magnetic field-responsive smart polymer
354 composites, *Adv Polym Sci*, 206 (2007) 137-189.
- 355 [15] Z. Varga, G. Filipcsei, M. Zrinyi, Smart composites with controlled anisotropy, *Polymer*, 46 (2005)
356 7779-7787.
- 357 [16] P.G. Yang, M. Yu, H.P. Luo, J. Fu, H. Qu, Y.P. Xie, Improved rheological properties of dimorphic
358 magnetorheological gels based on flower-like carbonyl iron particles, *Appl Surf Sci*, 416 (2017) 772-780.

359 [17] J.D. Carlson, M.R. Jolly, MR fluid, foam and elastomer devices, *Mechatronics*, 10 (2000) 555-569.
360 [18] X.H. Liu, Z.M. Fu, X.Y. Yao, F. Li, Performance of Magnetorheological Fluids Flowing Through
361 Metal Foams, *Meas Sci Rev*, 11 (2011) 144-148.
362 [19] X.H. Liu, P.L. Wong, W. Wang, W.A. Bullough, Feasibility Study on the Storage of
363 Magnetorheological Fluid Using Metal Foams, *J Intel Mat Syst Str*, 21 (2010) 1193-1200.
364 [20] F. Scarpa, F.C. Smith, Passive and MR fluid-coated auxetic PU foam - Mechanical, acoustic, and
365 electromagnetic properties, *J Intel Mat Syst Str*, 15 (2004) 973-979.
366 [21] L.C. Davis, Model of magnetorheological elastomers, *J Appl Phys*, 85 (1999) 3348-3351.
367 [22] M. Farshad, A. Benine, Magnetoactive elastomer composites, *Polym Test*, 23 (2004) 347-353.
368 [23] I. Bica, E.M. Anitas, M. Bunoiu, B. Vatzulik, I. Juganaru, Hybrid magnetorheological elastomer:
369 Influence of magnetic field and compression pressure on its electrical conductivity, *J Ind Eng Chem*, 20
370 (2014) 3994-3999.
371 [24] L. Chen, X.L. Gong, W.H. Li, Microstructures and viscoelastic properties of anisotropic
372 magnetorheological elastomers, *Smart Mater Struct*, 16 (2007) 2645-2650.
373 [25] M.R. Jolly, J.D. Carlson, B.C. Munoz, T.A. Bullions, The magnetoviscoelastic response of elastomer
374 composites consisting of ferrous particles embedded in a polymer matrix, *J Intel Mat Syst Str*, 7 (1996)
375 613-622.
376 [26] Y. Shen, M.F. Golnaraghi, G.R. Heppler, Experimental research and modeling of magnetorheological
377 elastomers, *J Intel Mat Syst Str*, 15 (2004) 27-35.
378 [27] T. Shiga, A. Okada, T. Kurauchi, Magnetroviscoelastic Behavior of Composite Gels, *J Appl Polym*
379 *Sci*, 58 (1995) 787-792.
380 [28] X.C. Guan, X.F. Dong, J.P. Ou, Magnetostrictive effect of magnetorheological elastomer, *J Magn*
381 *Magn Mater*, 320 (2008) 158-163.
382 [29] J.K. Wu, X.L. Gong, Y.C. Fan, H.S. Xia, Anisotropic polyurethane magnetorheological elastomer
383 prepared through in situ polycondensation under a magnetic field, *Smart Mater Struct*, 19 (2010).
384 [30] I.A. Perales-Martinez, L.M. Palacios-Pineda, L.M. Lozano-Sanchez, O. Martinez-Romero, J.G.
385 Puente-Cordova, A. Elias-Zuniga, Enhancement of a magnetorheological PDMS elastomer with carbonyl
386 iron particles, *Polym Test*, 57 (2017) 78-86.
387 [31] M. D'Auria, D. Davino, R. Pantani, L. Sorrentino, Polymeric foam-ferromagnet composites as smart
388 lightweight materials, *Smart Materials and Structures*, 25 (2016).
389